High Efficient Transparent TiO$_2$ Nanotube Dye-Sensitized Solar Cells: Adhesion of TiO$_2$ Nanotube Membrane to FTO by Two Different Methods

F. Mohammadpour[a], M. Moradi[a,b,*]

[a]*Department of Physics, College of Sciences, Shiraz University, Shiraz 71454, Iran*
[b]*Institute of Nanotechnology, Shiraz University, Shiraz 71454, Iran*

Abstract

In order to fabricate transparent TiO$_2$ nanotube dye-sensitized solar cells, anodically growth nanotube membranes are detached from Ti substrate by a re-anodization method. The membranes are transferred on FTO glass by two different methods. At the first one, 100mM Ti-isopropoxide is used to make TiO$_2$ nanoparticles for adhering TiO$_2$ nanotube membranes to FTO and in the second one a commercial TiO$_2$ nanoparticle paste is used as connector material. In order to investigate the effect of annealing temperature on the crystallinity of the photoanodes, they were annealed in temperatures from 350 to 650°C. All of the annealed photoanodes show high crystallinty and pure anatase phase in both cases. However nanoprticles with large diameter about 500nm and no homogeneity of dispersion of them at the first method leads to week interconnection between membranes and FTO glasses but good interconnection at the second method leads to high power conversion efficiency of 6.13% under 1 sun illumination without any extra treatment.

1. Introduction

Over the past decades, dye-sensitized solar cells (DSSC) have received considerable attention due to high efficiency and low cost [1,2]. However DSSC with a thick TiO$_2$ mesoporous film has been demonstrated high power conversion efficiency with optimizing dye molecules and electrolyte composition [3], but random walk of electrons between interconnected nanoparticles limit the electron transport time in these structures [4, 5]. In order to overcome this effect, one dimensional structures such as nanowires [6, 7], nanorods [8, 9] and nanotubes [10-12] are suggested. Among these nanostructures TiO$_2$ nanotubes are more considerable due to higher surface area than compact oxide film that leads to higher dye loading

and consequently more light harvesting efficiency [13].

Anodically growth TiO_2 nanotubes are amorphous in nature but can be converted to crystalline phases of rutile or anatase by annealing process [14-17]. Since the electron transport is faster in anatase in comparison to rutile phase [18,19], it is tried to omit rutile phase for using TiO_2 nanotubes in photovoltaic applications. However it is possible to omit rutile phase in low temperature by ramping annealing, but high temperature annealing usually leads to some percent of rutile phase. This effect can be removed by annealing the membrane after detaching from Ti substrate and transferring on FTO glass in the case of DSSCs.

Front side illumination is another benefit of this approach. The highest power conversion efficiency of a pure TiO_2 structure, without $TiCl_4$ treatment, on Ti foil is reported 5.2% to now [20]. One of the reasons that limits transport time and increasing power conversion efficiency in TiO_2 nanotube DSSCs is the existence of Ti foil beneath TiO_2 nanotubes that excludes front side illumination. Some parts of incident light to cell reflected by Pt cathode and some parts of it absorbs by iodine electrolyte. Some groups have tried to transfer TiO_2 nanotube on FTO substrate to have front side illumination [21-23].

In the present work, we prepare TiO_2 nanotube membranes [23] and transfer them on fluride-doped tin oxide (FTO) coated glasses to apply them to front side illuminated DSSC configurations. We use two different methods for adhesion of TiO_2 nanotube membranes to FTO glasses and compare the effect of them on the photovoltaic characteristics of transparent DSSCs.

2. Experimental procedure

Highly ordered TiO_2 nanotube arrays were prepared by anodization of Ti foil (0.125mm thickness, 99.7% purity, Advent) in a two electrode cell by using Pt as counter electrode. Prior to the anodization process the Ti foil was cleaned by sonication in acetone and ethanol followed by rinsing in de-ionized water (DI) and drying under N_2 stream. The anodization was performed at 60V at room temperature in a solution of ethylene glycol with 0.15 M NH_4F and 3V% water. Different TiO_2 nanotube thicknesses were produced by changing the anodization time from 10min to 60min. For producing TiO_2 nanotube membranes, the as-prepared TiO_2 nanotube samples were annealed in 350° C for 1h. The crystallized TiO_2 nanotube samples were anodized again in the first anodization conditions. The ordered TiO_2 nanotubes membrane was prepared by immersing the samples in 0.07 M HF solution at 30° C. The freestanding TiO_2 nanotube membranes were attached on FTO glasses (7 Ω per square) by two different methods. At the first method three drops of 100 mM Ti-isopropoxide [24] were applied on FTO glass and TiO_2 nanotube membrane was transferred on it. At the second method a commercial TiO_2 nanoparticle paste (Ti-Nanoxide HT, Solaronix) was coated on FTO glass by doctor-blade technique and membrane was transferred on it. In both cases, after drying the photoanodes in air for about 20 min, they were annealed in the range of 350-650 $^\circ$ C for 1h in a tube furnace.

The annealed photoanodes in 550° C were immersed in a 300 µM dye solution (D719, Everlight, Taiwan) at 40° C for 24h. After dye-sensitization the samples were rinsed with acetonitrile to remove non-chemisorbed dye and dried in N_2 stream. Then the photoanodes were sandwiched with a Pt coated FTO glass as a

counter electrode using a hot-melt spacer (25 µm, Surlyn, Dupont). Electrolyte (Io-li-tec, ES-0004) was introduced between the interspace of the DSSCs. The current voltage characteristics were measured under simulated AM 1.5 illumination provided by a solar simulator (300W Xe with an optical filter, Solarlight) applying an external bias to the cell and measuring the generated photocurrent with a Keithley model 2420 digital source meter.

For morphological characterization, a field-emission scanning electron microscope (FE-SEM, Hitachi SEM FE 4800) were used. X-ray diffraction analysis (XRD) was performed with an X'pert Philips MPD with a PanalyticalX´celerator detector using graphite monochromized Cu Kα radiation (wavelength 1.54056A°).

3. Results and discussion

Figure 1 (a-d) shows cross sectional SEM images of freestanding TiO_2 NT membranes with different thicknesses. The insets show back side of the membranes. It can be seen from these figures
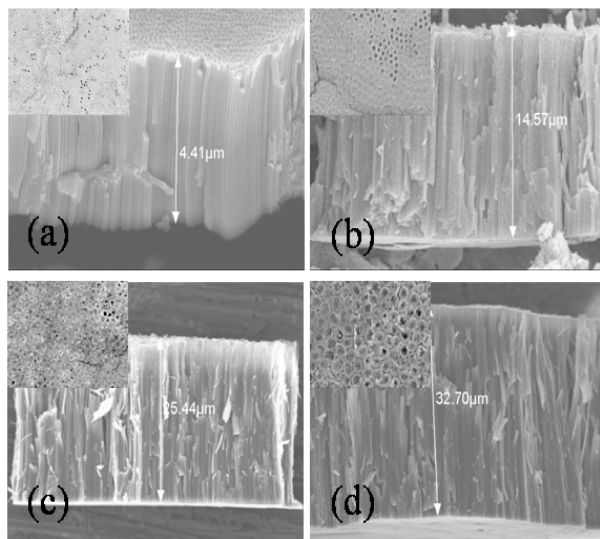
**Fig. 1.** The FE-SEM images (a-d) of TiO_2 nanotubes with thicknesses from 4 to 30 µm, the insets show back side of the membranes.
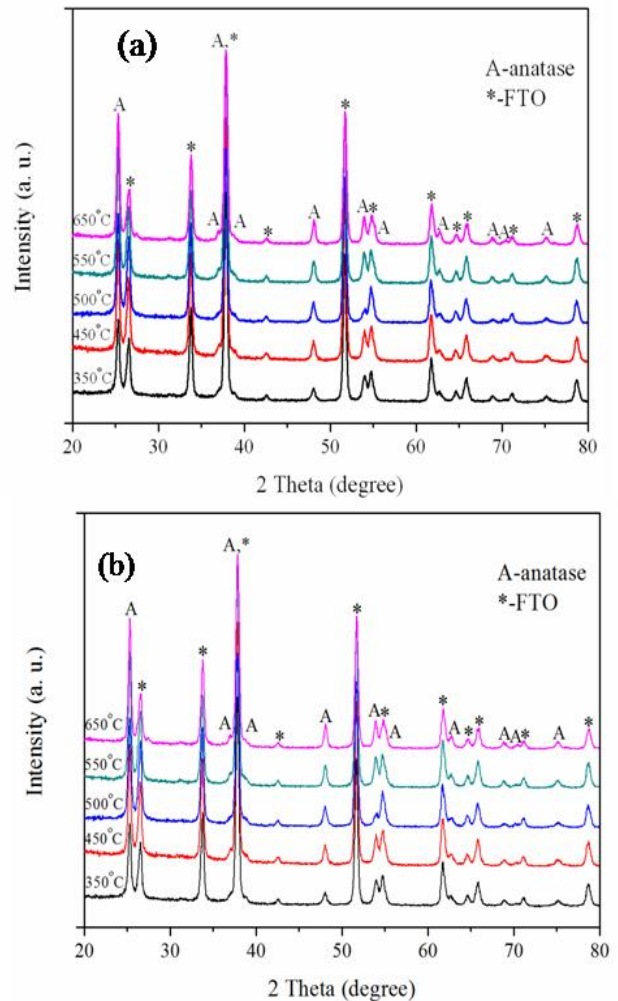
Fig. 2. XRD pattern of 20µm nanotube membrane annealed in temperatures from 350 to 650°C attached on FTO by Ti-isopropoxide method (a) and by 2µm commercial nanoparticle paste (b).

that the bottom of the tubes are opened in some parts.

To investigate the effect of annealing temperature on crystallinty of the tubes, two different configurations were annealed in air at temperatures from 350 to 650°C. Figure 2(a-b) show crystallinty of the tubes in 350 to 650°C.
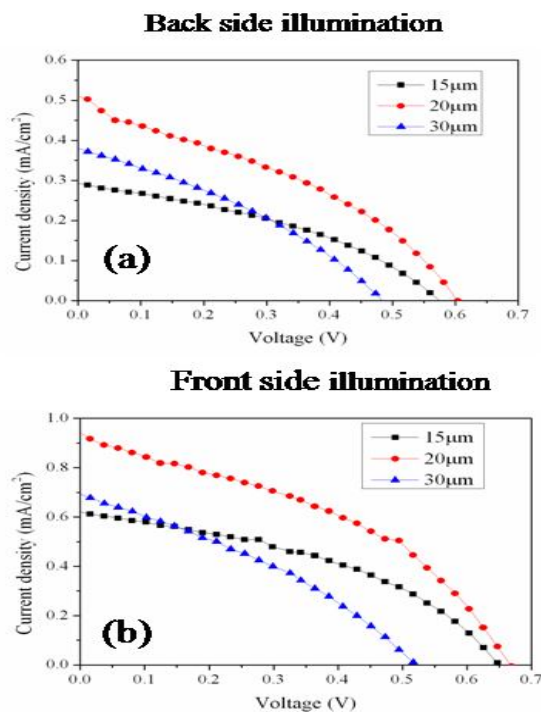
Fig. 3. (a, b) The J-V curves of DSSCs consisted of different thicknesses of TiO_2 nanotube membranes attached on FTO by Ti-isopropoxide method and annealed in $550^{\circ}C$.

Fig. 4. Schematic representation of back side (a) and front side (b) illumination in transparent TiO_2 nanotube DSSCs.

Table 1. The photovoltaic parameters of DSSCs consisted of different thicknesses of TiO_2 nanotube membranes attached on FTO by Ti-isopropoxide method and annealed in $550^{\circ}C$.
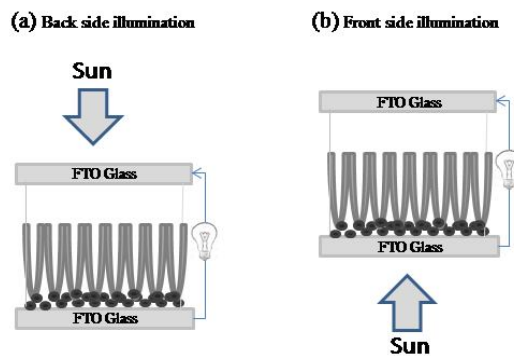
Back side illumination:

Tube Thickness	V_{oc}	I_{sc}	$\eta(\%)$	ff(%)
15μm	0.57	0.29	0.05	30
20μm	0.60	0.51	0.11	36
30 μm	0.49	0.37	0.05	27

Front side illumination:

| Tube Thickness	V_{oc}	I_{sc}	$\eta(\%)$	ff(%)
15μm	0.65	0.60	0.17	43
20μm	0.66	0.92	0.23	38
30 μm	0.52	0.69	0.12	33

These two kinds of illumination are schematically shown in Fig. 4.

Table 1 shows that however the open circuit voltages are enough high but low short circuit currents leads to low power conversion efficiencies in this method. The highest power conversion efficiency is 0.23% that is occurred in 20µm tubes. This power conversion efficiency is very low even with comparison to TiO_2 nanotubes on foil. Low current density might be because of weak interconnection between TiO_2 nanotube membrane and FTO glass. In order to remove this effect a commercial TiO_2 nanoparticle paste was used.

Figure 5 shows the photovoltaic characteristics of DSSCs consisted of different thicknesses of TiO_2 nanotube membranes on 2 µm nanoparticle paste. Similar to the previous one, the photoanodes are annealed at $550^{\circ}C$. As can be seen from this figure, however the open circuit voltages are in the same order of the Ti-isopropoxide case but short circuit currents are considerably more. This high J_{sc} and also high fill factor leads to high power conversion efficiency in this case. So that a high power conversion efficiency of 6.13% in 20 µm nanotube membrane in front side illumination is occurred. This power conversion efficiency is very high without any $TiCl_4$ treatment in comparison to DSSCs consisted of TiO_2 nanotubes on foil.
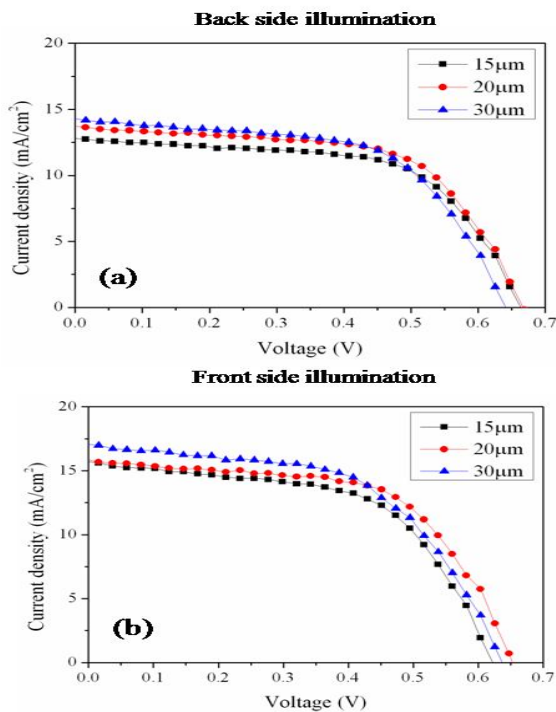
Fig. 5. (a, b) The J-V curves of DSSCs consisted of different TiO$_2$ nanotube array on 2µm nanoparticle paste annealed in 550°C.

Table 2. The photovoltaic parameters of DSSCs consisted of different thicknesses of TiO$_2$ nanotube array on 2µm nanoparticle paste annealed in 550°C.

Back side illumination:

| Tube Thickness	V_{oc}	I_{sc}	$\eta(\%)$	ff(%)
15µm	0.57	0.29	0.05	30
20µm	0.60	0.51	0.11	36
30 µm	0.49	0.37	0.05	27

Front side illumination:

Tube Thickness	V_{oc}	I_{sc}	$\eta(\%)$	ff(%)
15µm	0.65	0.60	0.17	43
20µm	0.66	0.92	0.23	38
30 µm	0.52	0.69	0.12	33

It can be concluded that 20 µm is an optimized thickness for the membranes in transparent DSSCs. Table 2 shows that however increment in thickness leads to higher J$_{sc}$ because of more dye-loading and

consequently higher light harvesting efficiency but decrement of V$_{oc}$ and fill factor resulted to lower power conversion efficiency.

Figure 6(a) shows the nanoparticles that are produced by Ti-isopropoxide method. It can be understood that big diameter of nanoparticles between 400 nm to 500 nm and weak homogeneity of dispersion of them can be resulted in weak interconnection between membranes and FTO glasses. As can be seen in figure 6(b), nanoparticles with diameter of 10 nm in the commercial paste lead to a compact and good interconnection between TiO$_2$ nanotube membranes and FTO glasses.
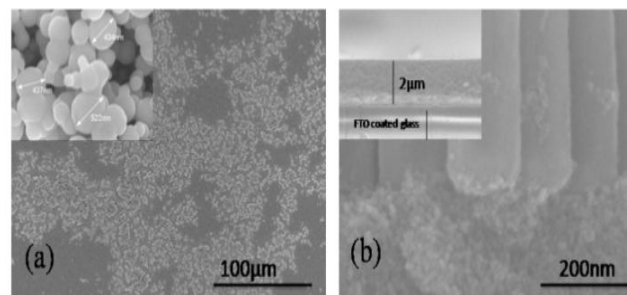
Fig. 6. FE-SEM images of nanoparticles is made by Ti-isopropoxide method (a), TiO$_2$ nanotubes on 2µm commercial nanoparticle paste (b). High magnifications are shown in the insets.

4. Conclusion

In the present work we detached TiO$_2$ nanotube membranes from Ti substrate by re-anodization method. The detached membranes are transferred on FTO glasses by two different methods. At first we used 100 mM Ti-isopropoxide to make TiO$_2$ nanoparticles as connector between membrane and FTO glass. Nanoparticles with large diameter about 500 nm and non-homogeneityof dispersion of them resulted to low short circuit current density and subsequently low power conversion efficiency. In comparison a commercial TiO$_2$ nanoparticle

paste with diameter about 10 nm as connector leaded to high J_{sc} and power conversion efficiency of 6.13% without any $TiCl_4$ treatment. Annealed photoanodes in different temperatures show pure anatase phase in both cases.

References

[1]   B. O'Regan, M. Grätzel, Nature 353(1991) 737.

[2] M. Grätzel, Journal of Photochemistry and Photobiology A 164 (2004) 3-8.

[3] J.H. Yum, E. Baranoff, F. Kessler, T. Moehl, S. Ahmad, T. Bessho, A. Marchioro, E. Ghadiri, J.E. Moser, C. Yi, M.K. Nazeeruddin, M. Grätzel, J. Nat. Commun. 3 (2012) 631-637.

[4] J. Nelson, Phys. Rev. Lett. B: Condens. Matter. 59 (1999) 15374. A. Ghicov, P. Schmuki, Chem. Commun. (2009) 2791-2796.

[5] J. Bisquert, Phys. Rev. Lett. 91 (2003) 010602.

[6] Q. Shen, T. Sato, M. Hashimoto, C. Chen, T. Toyoda. Thin Solid Films 499 (2006) 299-305.

[7] M. Adachi, Y. Murata, J. Takao, J. Jiu, M. Sakamoto, F. Wang, J. American Chemical Society 126 (2004) 14943-14950.

[8] S.H. Kang, S.-H. Choi, M.-S.Kang, J.-Y.Kim, H.-S. Kim, T. Hyeon, Y.E. Sung, Advanced Materials 20 (2008) 54-60.

[9] S. Pavasupree, S. Ngamsinlapasathian, Y. Suzuki, S. Yushikawa. J. Nanoscience and Nanotechnology 6 (2006) 3685-3692.

[10] A. Ghicov, S. Albu, R. Hahn, D. Kim, T. Stergiopoulos, J. Kunze, C.–A. Schiller, P. Falaras, P. Schmuki. Chemistry, An Asian Journal 4 (2009) 520-528.

[11] P. Roy, D. Kim, K. Lee, E. Spiecker, P. Schmuki. Nanoscale 2 (2010) 45-53.

[12] J.M. Macak, H. Tsuchiya, A. Ghicov, P. Schmuki. J. Electrochem. Commun. 7 (2005) 1133-1140.

[13] K. Zhou, N.R. Neale, A. Miedaner, A. Frank. J. Nano. Lett. 7 (2007) 69-76.

[14] J.M. Macak, K. Sirotna, P. Schmuki. Electrochim. Acta. 50 (2005) 3679-3685.

[15] R. Beranek, H. Tsuchia, T. Sugishima, J.M. Macak, L. Taveria, S. Fujimoto, H. Kisch, P. Schmuki. J. Appl. Phys. Lett. 87 (2005) 243114-243120.

[16] A. Tighineanu, T. Ruff, S.P. Albu, R. Hahn, P.Schmuki. Chem. Phys. Lett. 494 (2010) 260-272.

[17] A. Ghicov, H. Tsuchiya, J.M. Macak, P. Schmuki. Phys. Status. Solidi A. 203 (2006) R28.

[18] H. Tang, K. Prasad, R. Sanjinbs, P.E. Schmit, F.J. Levy. Appl. Phys. 75 (1994) 2042-2050.

[19] A. Ghicov, S.P. Albu, R. Hahn, D. Kim, T. Stergiopoulos, J. Kunze, C.A. Schiller, P. Falaras, P. Schmuki. J. Chem. Asian 4 (2009) 520-528.

[20] P. Roy, S.P. Albu, P. Schmuki. J. Electrochem. Commun. 12 (2010) 949-956.

[21] Q. Chen, D. Xu. J. Phys. Chem. C 113 (2009) 6310-6316.

[22] K. H. Chung, M. M. Rahman, H. S. Son, J.J. Lee. International Journal of Photoenergy 2012 (2012) 215802-215810

[23] M. Dubey, M. Shrestha, Y. Zhong, D. Galipeau, H. He. Nanotechnology 22 (2011) 285201-285209

[24] J.H. Park, T.W. Lee, M.G. Kang. J. Chem. Commun. (2008) 2867-2872.